Original Article

MOLECULAR METABOLISM

An early, reversible cholesterolgenic etiology of diet-induced insulin resistance

Jacob D. Covert [1,3,8], Brian A. Grice [1,3,8], Matthew G. Thornburg [1,3,8], Manpreet Kaur [1,3], Andrew P. Ryan [1,3,4], Lixuan Tackett [1,3], Theja Bhamidipati [1,3], Natalie D. Stull [5], Teayoun Kim [6], Kirk M. Habegger [6], Donald A. McClain [7], Joseph T. Brozinick [1,3,6], Jeffrey S. Elmendorf [1,2,3,*]

ABSTRACT

Objective: A buildup of skeletal muscle plasma membrane (PM) cholesterol content in mice occurs within 1 week of a Western-style high-fat diet and causes insulin resistance. The mechanism driving this cholesterol accumulation and insulin resistance is not known. Promising cell data implicate that the hexosamine biosynthesis pathway (HBP) triggers a cholesterolgenic response via increasing the transcriptional activity of Sp1. In this study we aimed to determine whether increased HBP/Sp1 activity represented a preventable cause of insulin resistance.

Methods: C57BL/6NJ mice were fed either a low-fat (LF, 10% kcal) or high-fat (HF, 45% kcal) diet for 1 week. During this 1-week diet the mice were treated daily with either saline or mithramycin-A (MTM), a specific Sp1/DNA-binding inhibitor. A series of metabolic and tissue analyses were then performed on these mice, as well as on mice with targeted skeletal muscle overexpression of the rate-limiting HBP enzyme glutamine-fructose-6-phosphate-amidotransferase (GFAT) that were maintained on a regular chow diet.

Results: Saline-treated mice fed this HF diet for 1 week did not have an increase in adiposity, lean mass, or body mass while displaying early insulin resistance. Consistent with an HBP/Sp1 cholesterolgenic response, Sp1 displayed increased *O*-GlcNAcylation and binding to the HMGCR promoter that increased HMGCR expression in skeletal muscle from saline-treated HF-fed mice. Skeletal muscle from these saline-treated HF-fed mice also showed a resultant elevation of PM cholesterol with an accompanying loss of cortical filamentous actin (F-actin) that is essential for insulin-stimulated glucose transport. Treating these mice daily with MTM during the 1-week HF diet fully prevented the diet-induced Sp1 cholesterolgenic response, loss of cortical F-actin, and development of insulin resistance. Similarly, increases in HMGCR expression and cholesterol were measured in muscle from GFAT transgenic mice compared to age- and weight-match wildtype littermate control mice. In the GFAT Tg mice we found that these increases were alleviated by MTM.

Conclusions: These data identify increased HBP/Sp1 activity as an early mechanism of diet-induced insulin resistance. Therapies targeting this mechanism may decelerate T2D development.

Keywords Cholesterol; Insulin resistance; Membrane; Skeletal muscle

1. INTRODUCTION

From a public health standpoint, understanding the pathophysiological changes that lead to insulin resistance at the earliest possible stage would have far-reaching implications in decelerating the enormous worldwide incidence of type 2 diabetes (T2D). In its earliest phases, a major feature of this disease is skeletal muscle insulin resistance, which is of considerable importance since skeletal muscle is responsible for the disposal of the majority of an exogenous glucose load [1]. We found that early insulin resistance in mice fed a Western-style high fat (HF) for 1 week is caused by increased skeletal muscle plasma membrane (PM) cholesterol and loss of cortical filamentous

[1]Department of Anatomy, Cell Biology and Physiology, Indianapolis, IN, United States [2]Department of Biochemistry and Molecular Biology, Indianapolis, IN, United States [3]Center for Diabetes and Metabolic Diseases, Indiana University School of Medicine, Indianapolis, IN, United States [4]Eli Lilly and Company, Indianapolis, IN, United States [5]Indiana Biosciences Research Institute Indianapolis, IN, United States [6]Comprehensive Diabetes Center and Department of Medicine, Division of Endocrinology, Diabetes, and Metabolism, University of Alabama at Birmingham, Birmingham, AL, United States [7]Section of Endocrinology and Metabolism, Wake Forest School of Medicine, Winston-Salem, NC, United States

[8] Jacob D. Covert, Brian A. Grice, Matthew G. Thornburg contributed equally to this work.

*Corresponding author. Department of Anatomy, Cell Biology & Physiology, Department of Biochemistry & Molecular Biology, Center for Diabetes Research & Metabolic Diseases, Indiana University School of Medicine, Van Nuys Medical Science Building, Rm. 307, Indianapolis, IN 46202, United States. Fax: +1 317 274 3318. E-mail: jelmendo@iupui.edu (J.S. Elmendorf).

Abbreviations: EE, Energy expenditure; F-actin, Filamentous actin; GFAT, Glutamine:fructose-6-phosphate amidotransferase; GIR, Glucose infusion rate; GLUT4, Insulin-responsive glucose transporter; HBP, Hexosamine biosynthesis pathway; HF, High-fat; HMGCR, Hydroxy-3-methylglutaryl CoA reductase; HPRT, Hypoxanthine phosphoribosyl transferase; LF, Low-fat; MTM, Mithramycin-A; PM, Plasma membrane; R_a, Endogenous glucose production; R_d, Glucose disposal; R_g, Glucose uptake; RER, Respiratory exchange ratio; SAL, Saline; SC, Standard chow; Sp1, Specificity protein 1; SPA, Spontaneous physical activity; T2D, Type 2 diabetes; Tg, Transgenic; VCO_2, Carbon dioxide production; VO_2, Oxygen consumption; Wt, Wildtype

Received December 15, 2022 • Revision received February 27, 2023 • Accepted March 21, 2023 • Available online 3 April 2023

https://doi.org/10.1016/j.molmet.2023.101715

actin (F-actin) [2], an actin network that is essential for insulin-regulated glucose transport [3–6]. Treatment of these mice with the cholesterol-lowering dextrin (MβCD) during the 1-week HF diet prevented muscle cholesterol buildup, F-actin loss, and insulin resistance [2]. These results identified excess skeletal muscle PM cholesterol as an early reversible cause of diet-induced insulin resistance.

These findings complement a growing volume of clinical data that increased intracellular cholesterol is a risk factor for T2D [7–10]. In agreement with these findings, we found that muscle biopsies from individuals across a range of insulin sensitivities have an inverse correlation between cholesterol content and glucose disposal [11]. The mechanism by which skeletal muscle cholesterol accumulates early in the setting of HF feeding is not known. An understanding would be rewarding as it may lead to novel approaches to prevent the development of insulin resistance. Some promising *in vitro* data revealed that *de novo* cellular cholesterol biosynthesis can be triggered by increased activity of the hexosamine biosynthesis pathway (HBP) [11–13], a pathway well recognized to play a fundamental role in the etiology of T2D [14–16]. We found that various cell culture conditions that increase HBP activity cause PM cholesterol accumulation, cortical F-actin loss, and insulin resistance [11–13]. We further found that MβCD normalization of excess PM cholesterol in these cells restored cortical actin filaments and prevented HBP-induced insulin resistance [11,13].

Essential features of the HBP include the first and rate-limiting enzyme, glutamine:fructose-6-phosphate-amidotransferase (GFAT), which converts fructose-6-phosphate and glutamine into glucosamine-6-phosphate (GlcN-6-P). GlcN-6-P is subsequently metabolized, culminating in the production of UDP-N-acetylglucosamine (UDP-GlcNAc), the high energy substrate for *O*-GlcNAc transferase (OGT), a nuclear and cytosolic enzyme that catalyzes the addition of GlcNAc to serine/threonine residues [17,18]. This posttranscriptional modification modulates the activities of signaling proteins, regulates most components of the transcription machinery, affects cell cycle progression, and regulates the targeting/turnover or functions of many other regulatory proteins [19–21]. Mice overexpressing GFAT [22,23] or OGT [24] in skeletal muscle and adipocytes develop peripheral insulin resistance as they age, without manifesting changes in body mass or expression of the insulin-responsive glucose transporter, GLUT4. The *in vivo* insulin resistance in these mice is associated with impaired insulin stimulated GLUT4 redistribution to the PM [22].

While many key insulin signaling proteins (e.g., *IRS1, PDK1, Akt, Munc18c*) are subject to *O*-GlcNAcylation [20], defects in their signaling do not account for HBP-mediated insulin resistance [16,25–27]. This was further confirmed by experiments in which overexpression of *O*-GlcNAcase, the enzyme that removes *O*-GlcNAc moieties from proteins was found to be ineffective in mitigating HBP-induced insulin resistance in 3T3-L1 adipocytes [26]. Notably, *O*-GlcNAcylation was decreased only in the cytosolic fraction of these cells, whereas in isolated nuclei, no significant increase in *O*-GlcNAcase activity was detected [26]. This is consistent with the postulate that nuclear proteins are critical *O*-GlcNAcylation targets that cause insulin resistance.

In 3T3-L1 adipocytes we found that *O*-GlcNAcylation of the transcription factor Sp1 leads to transcription of hydroxy-3-methylglutaryl CoA reductase (HMGCR) [12]. This HBP-induced transcriptional response increased PM cholesterol and decreased cortical F-actin, which impaired cellular insulin sensitivity [12]. Importantly, these *in vitro* analyses demonstrated that either inhibition of GFAT, or blockade of *O*-GlcNAc-modified Sp1 binding to DNA, prevented cellular cholesterol buildup, F-actin disruption, and insulin resistance [12]. Whether the excess membrane cholesterol content measured in insulin-resistant skeletal muscle from HF-fed mice results from increased HBP/Sp1 activity is not known. Herein, using mithramycin-A (MTM), a specific Sp1/DNA-binding inhibitor [12,28,29], we tested this possibility in HF-fed mice and mice with targeted overexpression of GFAT in skeletal muscle.

2. MATERIALS AND METHODS

2.1. Mice

Male C57BL/6NJ (6N) mice were obtained at 4–6 weeks of age from Jackson Laboratory, Bar Harbor, ME and were singly housed and maintained on a 12-h light/dark cycle. Male and female mice with targeted muscle overexpression of the rate limiting HBP enzyme GFAT [23] were group housed and fed a regular chow diet. The Indiana University School of Medicine (IUSM) and University of Alabama at Birmingham (UAB) Institutional Animal Care and Use Committee approved all animal protocols.

2.2. Diet and treatment intervention

Upon arrival to our facility, all mice had free access to water and standard chow (SC) for 1 week (see Figure 1). Following this 1-week facility acclimation period, all mice received a low-fat (LF) diet containing 20% kcal from protein, 70% kcal from carbohydrates, and 10% kcal from fat (D01030107, Research Diets Inc., New Brunswick, NJ) for 1 week to adapt to the modified diet. This LF, as well as the high-fat (HF), diet represented modified forms of the standard LF (D12450H) and HF (D12451) diets from Research Diets Inc., with an adaptation regarding type of fat (palm oil instead of lard), with the HF diet having a ratio of saturated to monounsaturated to polyunsaturated fatty acids of 40:40:20. Note that both diets contain approximately 0.2 mg cholesterol per gram of casein, an ingredient in these diets. Using this number, the estimated levels of cholesterol on a weight per weight basis in the LF and HF diets are 37.9 mg/kg and 46.6 mg/kg,

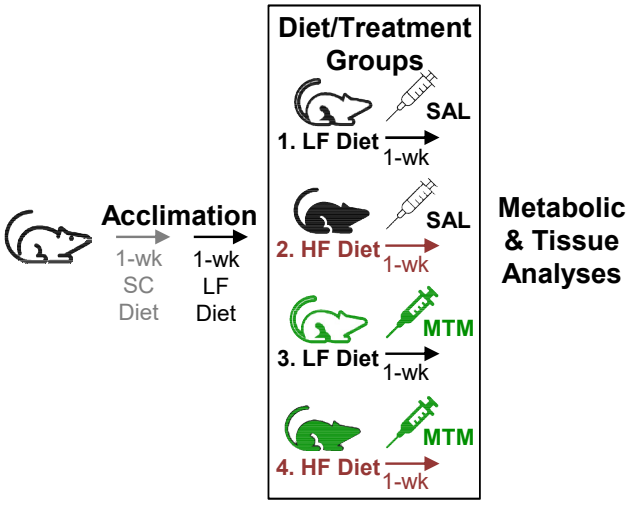

Figure 1: Dietary and treatment intervention plan. Upon arrival to our facility, 2 wks before the diet and treatment intervention all mice were singly housed, given standard laboratory chow (SC) for 1 wk and then the low-fat (LF) diet for 1 wk to adapt to the modified diet. Following this 2-wk acclimation period, mice were either left on the LF diet (Groups 1 and 3, black line) or switched to the HF diet (Groups 2 and 4, red line). Mice were injected intraperitoneally with either saline (SAL, Groups 1 and 2, black) or 0.15 mg/kg mithramycin-A (MTM, Groups 3 and 4, green) daily during the 1-week LF or HF diet. All groups consisted of several cohorts of 6–9 mice for metabolic/tissue analyses performed immediately following the 1-wk diet/treatment period.

respectively. Following this 2-week acclimation period, mice were either left on the LF diet (Figure 1, Groups 1 and 3) or switched to the HF diet (Figure 1, Groups 2 and 4) containing 20% kcal from protein, 35% kcal from carbohydrates, and 45% kcal from fat (D01030108). Mice were injected intraperitoneally (i.p.) with either saline (Figure 1, SAL, Groups 1 and 2) or 0.15 mg/kg mithramycin-A (Figure 1, MTM, Groups 3 and 4) daily during the 1-week LF or HF diet. We also treated male and female GFAT transgenic (Tg) and littermate wildtype (Wt) control mice with saline or MTM (i.p. 0.15 mg/kg/day/week). All groups consisted of several cohorts of 6–9 mice for metabolic/tissue analyses performed immediately following the 1-week intervention. Several previous studies and data we have collected permitted us to use power analysis to calculate/validate the number of animals needed for our major outcome variables, membrane cholesterol, actin, and glucose transport. For these studies, 6 mice per group was calculated to provide a statistical power of 85% using $\alpha = 0.05$.

2.3. Monitoring of activity, feeding and body composition

Mice were housed individually, and indirect calorimetry measures were performed using a TSE Systems PhenoMaster Metabolism Research Platform (Chesterfield, MO) equipped with calorimetry, feeding/drinking, and activity monitoring. Mice were monitored for 7 days under standard 12-h light/dark cycles. Oxygen consumption (VO_2) and carbon dioxide production (VCO_2) were monitored and VO_2 and VCO_2 levels were used to calculate the respiratory exchange ratio (RER). EchoMRI Body Composition Analyzer (EchoMRI, LLC, Houston, Texas) assessed body, lean and fat mass.

2.4. Assessment of glucose tolerance and insulin sensitivity

For the intraperitoneal glucose tolerance test, mice that were fasted for 5–6 h were administered glucose (2 g/kg i.p.). Tail vein blood glucose was measured at times indicated with an AlphaTRAK blood glucose meter (Abbott Laboratories, Inc. Alameda, CA). The integrated response to glucose for each individual animal was determined by calculating the area under the curve (AUC) by using each animal's baseline (time = 0 min) blood glucose measurement as previously described [30,31]. Hyperinsulinemic-euglycemic clamp studies were conducted as previously described [32,33]. In brief, catheters were implanted in mice following the 2-week SC and LF acclimation period (see Fig. 1). Mice were then maintained on the LF diet or placed on the HF diet and treated with saline or MTM as described above, and seven days postoperative, mice were fasted for 5 h. Insulin (4 mU/kg/min, diluted in 3% mouse plasma) was infused through the venous catheter, and euglycemia (90 mg/dL) was maintained by adjusting the infusion rate of a 50% glucose solution mixed with [3-^{3}H]-glucose 0.02 μCi/μl [34]. A tracer equilibration period (t = −120 to 0 min) was used as follows: a 1.6 μCi bolus of [3-^{3}H]-glucose (PerkinElmer, Boston, MA) was given at t = −120 min followed by a 0.04 μCi/min infusion for 2 h. Blood samples (100 μL) were taken at −120, −15, −5, 80, 90, 100, 110, 120, 122, 127, 135, 145, and 155 min for the assessment of glucose and insulin. Red blood cells from these samples were recovered by centrifugation and injected via arterial catheter to prevent a hematocrit deficit. At the end of the clamp, mice were euthanized, and tissues were snap frozen in liquid nitrogen. Plasma [3-^{3}H]-glucose and ^3H_2O were measured to determine rate of endogenous glucose production (R_a) and rate of glucose disposal (R_d) correcting for non-steady state conditions as previously described [35]. Plasma radioactivity and specific activity profiles for both the basal and clamp period are provided in Supplemental Fig. 1. Clamp plasma glucose was measured from 20 μL of deproteinized samples (Glucose Assay Kit; Cell Biolabs, San Diego, CA). Tissue-specific [3-^{3}H]-glucose incorporated glycogen was measured as previously reported [34]. Plasma insulin was measured using ultra-sensitive mouse insulin ELISA (Crystal Chem, Downers Grove, IL).

2.5. Protein and mRNA Sp1 and HMGR analyses

Mixed hindlimb skeletal muscle was rapidly harvested from mice immediately following the 1-week diet/treatment interventions (see Fig. 1). The muscles were trimmed off their tendons, blotted, and snap frozen in liquid nitrogen. Muscles were stored at −80 °C until processed to quantify GFAT protein expression, Sp1 binding to the HMGCR promoter, and HMGCR mRNA expression levels as we have previously detailed [2,12]. Note, for determination of *O*-GlcNAcylation of Sp1 presented in Figure 5, we used muscles from a cohort of 6 mice/group that were processed the same way and stored at −80 °C from a previous study using the same LF- and HF-fed mouse model [2].

2.6. Triad isolation and measurement of cholesterol content

Isolation of triad-enriched fractions from mixed hindlimb skeletal muscle was performed using differential centrifugation as previously reported [36]. Briefly, skeletal muscle was homogenized in ice-cold HES buffer with a Polytron PT-10 homogenizer 3 times in 10-second bursts. After homogenization the sample was centrifuged at 1380 g for 30 min. The supernatant was saved, and the pellet was resuspended and centrifuged at 1380 g for 30 min. The supernatant from the second centrifugation was combined with the supernatant from the first spin and centrifuged at 17,000 g for 30 min. The supernatant from this 17,000 g spin was discarded and the pellet was homogenized in HES buffer and centrifuged at 1380 g for 30 min. The pellet was discarded and the supernatant from this 1380 g spin was centrifuged at 17,000 g for 30 min. The resulting pellet was resuspended in 0.2 ml of HES buffer and stored at −80 °C for analysis. Cholesterol content was assayed using the Amplex Red Cholesterol Assay Kit (Molecular Probes), as we previously described [13]. We previously confirmed triad fraction purity using this differential centrifugation approach [2]. Equal protein loading was confirmed with the Revert Total Protein Stain (Li-Cor, Lincoln, NE).

2.7. Actin analyses

We dissected out soleus muscles from three mice per group. Muscles were quickly sliced into 1–3 thin (~1 mm) sections with a scalpel. Immunofluorescent labeling and imaging cortical F-actin was carried out as previously described [6]. Briefly, the thin sections were blotted on gauze, quickly rinsed in saline, and immersed in 4% paraformaldehyde/PBS. Following fixation for 2 h, the tissue sections were washed with PBS, then permeabilized for 20 min at room temperature in 0.2% Triton X-100/0.05% Tween 20/PBS. Tissue sections were rinsed three times in PBS then blocked in 5% donkey serum for 60 min at room temperature. Tissue sections were then incubated overnight at 4 °C in mouse anti-human F-actin antibody (MCA358G, Bio-Rad, Hercules, CA) diluted 1:50 in blocking buffer. Samples were washed extensively in PBS before incubation for 60 min at room temperature in 1:50 fluorescein-conjugated donkey anti-mouse IgM. Extensive washing in PBS and a quick ddH2O rinse followed secondary antibody incubations. Tissues were mounted on slides with Vectashield and were analyzed via confocal microscopy (LSM 510 NLO; Zeiss, Thornwood, NY). Prior to imaging, all samples were de-identified to ensure an objective analysis. All images were taken in the same focal plane of the section and under identical microscopic parameters. Images shown in Figure 6D are representative of 3–5 fields from each tissue section. Quantification shown in Figure 6E as a scatter dot plot shows each field imaged (3–5 fields per section per animal) as an individual dot.

2.8. Statistical analyses

Values presented are means ± SEM. The significance of differences between means was evaluated by unpaired t-tests, one-way ANOVA, or a two-way ANOVA where appropriate. Where a difference was indicated by ANOVA, Tukey's post-hoc test was conducted to compare differences between groups. GraphPad Prism 8 software was used for all analyses. $p < 0.05$ was considered significant.

3. RESULTS

3.1. Effects of diet and intervention on body composition, caloric intake, and glucose tolerance

We first examined the effect of mithramycin-A (MTM) on body composition, caloric intake, and glucose tolerance in mice fed and treated as described in Figure 1. Saline-treated HF-fed mice showed no significant change in body mass when compared to the saline-treated LF-fed mice (Figure 2A). We also observed no significant increase in lean mass or adiposity (Figure 2B,C) following the 1-week HF diet, nor did daily MTM treatment alter body composition (Figure 2A—C) or caloric intake (Figure 2D). However, 1 week of HF feeding significantly impaired glucose tolerance in saline-, but not MTM-, treated mice (Figure 2E,F). Note 2-way ANOVA analysis showed a main diet effect on body mass and caloric intake (Figure 2A,D; Dx $P < 0.05$).

3.2. Measurements of systemic and tissue insulin sensitivity

We next conducted hyperinsulinemic-euglycemic clamp studies. Glycemia was clamped to 90 mg/dL in all groups (Figure 3A) under similar levels of hyperinsulinemia (Figure 3B). Consistent with the glucose tolerance results, clamps uncovered a striking decrease in the glucose infusion rate (GIR) and the rate of glucose disposal (R_d) indicative of insulin resistance in the saline-treated HF-fed mice compared to the saline-treated LF-fed mice (Figure 3C—E). These decreases in both GIR and R_d were completely prevented in MTM-treated HF-fed mice. In accordance with whole body improvement of glucose disposal, gastrocnemius (Gastroc), soleus, and tibias anterior (TA) skeletal muscle [^{14}C]-2DG uptake were enhanced in MTM-treated HF-fed mice (Figure 3F). We did not observe a diet or MTM effect of brown adipocyte tissue (BAT) [^{14}C]-2DG uptake (Figure 3F). Insulin-stimulated suppression of endogenous glucose production (R_a) was observed in all groups. However, this suppression was greater in saline- and MTM-treated LF-fed mice and MTM-treated HF-fed mice as compared to saline-treated HF-fed mice (Figure 3G). These data show that HF feeding impaired hepatic insulin action and MTM treatment reversed this defect. Muscle glycogen synthesis was specifically elevated by MTM treatment (Figure 3I), consistent with MTM restoring R_d (see Figure 3E) in muscle. In the liver, no diet or intervention effect on glycogen synthesis was observed (Figure 3H). These data are consistent with a protective effect of MTM on skeletal muscle and liver insulin resistance.

3.3. Effects of diet and intervention on metabolic function and energy expenditure

Mice fed a HF diet for 1 week did not show a diet-induced change in light- or dark-phase oxygen consumption, carbon dioxide production, or spontaneous physical activity, yet did show a main diet-induced decrease in light- and dark-phase respiration (Figure 4A—D). All these measurements, except respiration for the saline-treated LF- and HF-fed and MTM-treated HF-fed mice were higher in the dark-phase. While post hoc analyses revealed no effect of MTM on light- or dark-phase oxygen consumption, carbon dioxide production, respiration, or spontaneous physical activity in either the LF-fed mice or HF-fed mice, a main treatment effect of slightly lowering light-phase oxygen consumption and carbon dioxide production was measured (Figure 4A,B). There was no main treatment effect on light- or dark-phase respiration and spontaneous physical activity (Figure 4C,D). As shown in Figure 4E,F, a slight decrease in energy expenditure was associated with MTM treatment, despite unaffected caloric intake or spontaneous physical activity (see Figures 2D and 4D).

3.4. Effects of diet and intervention on the HBP/Sp1-mediated cholesterolgenic response

Increased skeletal muscle membrane cholesterol drives early systemic insulin resistance in our HF-fed mice [2]. Likewise, HBP-mediated *O*-GlcNAcylation of Sp1 induces insulin resistance in 3T3-L1 adipocytes by activating a cholesterolgenic response [12]. Prior to beginning this current study, we first probed whether *O*-GlcNAcylation of Sp1 occurred in skeletal muscle we had stored at −80 °C from our previous study using this same LF- and HF-fed mouse model [2]. Consistent with our *in vitro* findings, immunoprecipitated Sp1 from skeletal muscle revealed increased RL2-antibody detection of Sp1 *O*-GlcNAcylation from HF-fed mice compared to LF-fed mice (Figure 5A). We confirmed this observation by subjecting skeletal muscle Sp1 immunoprecipitates to enzymatic biotin labeling of *O*-GlcNAc (Figure 5B), as we have previously reported [12]. Consistent with *O*-GlcNAcylation of Sp1 increasing its transcriptional activity [12], chromatin immunoprecipitation of Sp1 uncovered increased binding of Sp1 to the HMGCR promoter in skeletal muscle from saline-treated HF-fed mice compared to saline-treated LF-fed mice ($P = 0.0538$) that was fully prevented by MTM (Figure 6A). Figure 6B,C shows that increased Sp1 binding to the HMGCR in skeletal muscle from saline-, but not MTM-, treated HF-fed mice was associated with increased HMGCR mRNA expression and membrane cholesterol content. In addition, this was associated with an averted loss of cortical actin filaments visualized in saline-, but not MTM-, treated HF-fed mice (Figure 6D,E). Note, as detailed under "Material & Methods", we visualized cortical F-actin in thin (∼1 mm) soleus muscle sections (Figure 6D). To quantitate, we made a multiple number of measures on F-actin intensity/area in soleus muscle sections prepared from 3 separate mice per experimental group (Figure 6E). Collectively, these findings are consistent with a reversible Sp1-mediated cholesterolgenic response causing early diet-induced insulin resistance.

3.5. Effect of GFAT overexpression on skeletal muscle cholesterol and glucose tolerance

Because we have demonstrated that increased Sp1 transcriptional activity can be triggered by the HBP [12], we next used a transgenic mouse model that overexpresses GFAT, the rate-limiting HBP enzyme, and displays defective insulin-stimulated GLUT4 regulation and glucose disposal [22,23]. Using Tg and Wt littermate controls that did not differ in age or body mass (Figure 7A) and showed targeted overexpression of GFAT in skeletal muscle (Figure 7B), we measured a significant increase in skeletal muscle cholesterol (Figure 7C). Figure 8A,B shows similar body mass of a second cohort of age- and weight-matched male and female Tg and Wt littermate control mice we treated with either saline or MTM for 1 week. Figure 8C,D correspondingly show that skeletal muscle HMGCR mRNA expression and PM cholesterol were increased in saline-, but not MTM-, treated Tg mice. Whereas elevated skeletal muscle cholesterol was measured in male Tg mice consistent with the increased HMGCR expression, we did not have enough female mice to assess HMGCR expression. Also, while we did not perform a hyperinsulinemic-euglycemic clamp on

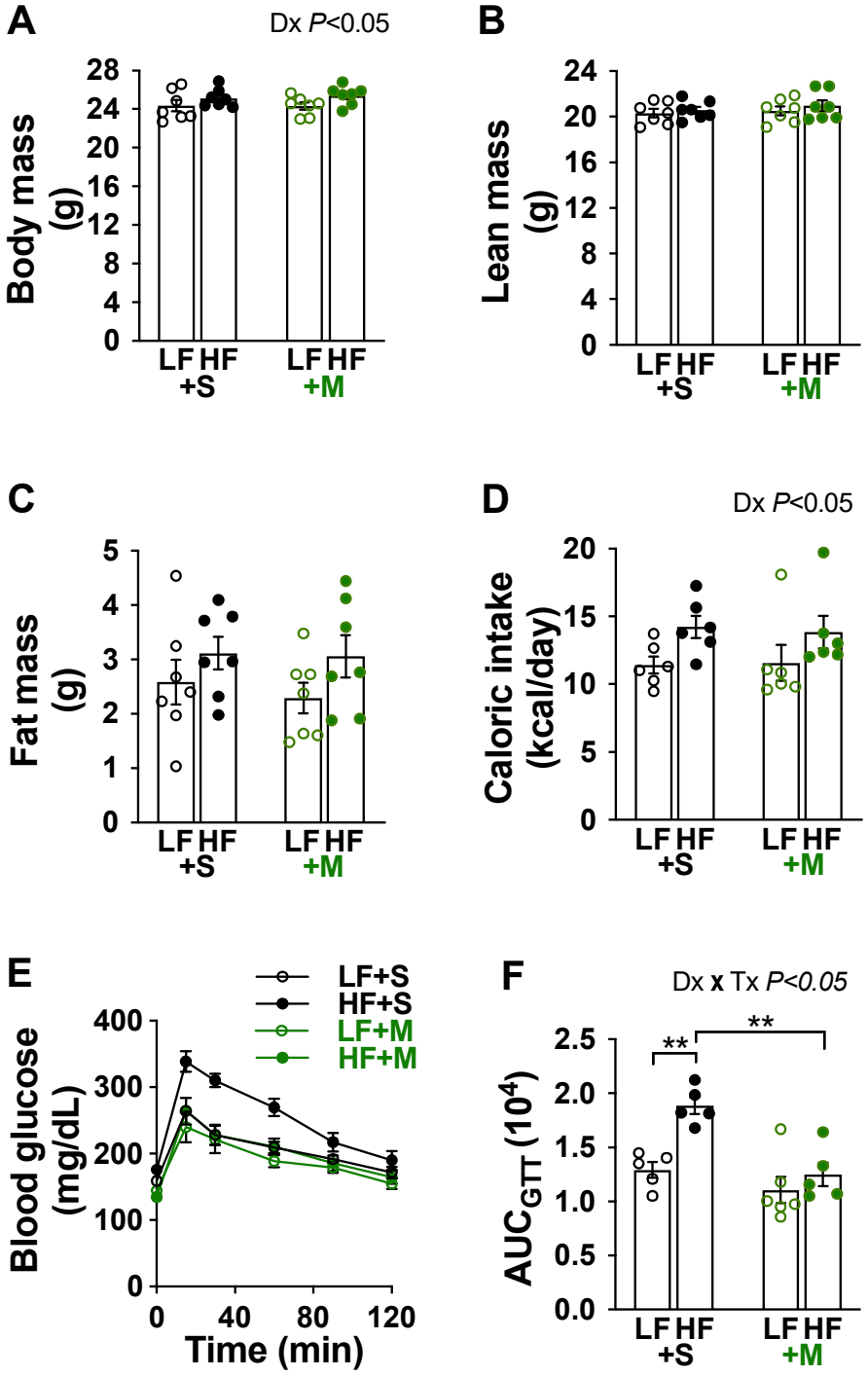

Figure 2: High-fat feeding for 1 week impaired glucose tolerance in saline-, but not MTM-, treated mice. (A–C) Body mass, lean mass, and adiposity following the 1-wk diet/treatment intervention for LF- (open symbols) and HF-fed (solid symbols) mice treated daily during the intervention with saline (black symbols) or MTM (green symbols) (n = 7 per group). (D) Average daily caloric intake during the 1-wk diet/treatment intervention (n = 6 per group). (E) Blood glucose measured after an intraperitoneal injection of glucose (2 g/kg, n = 5–6 per group). (F) Area under the curve (AUC). Data represent means ± SEM. Difference between groups was analyzed using a two-way ANOVA and Tukey's multiple comparison tests. $^{**}p < 0.005$.

these mice in this study to assess insulin sensitivity, previous use of this technique confirmed insulin resistance in male and female Tg mice [23]. In summary, these data support that increased HBP activity known to cause insulin resistance stimulates the Sp1 cholesterolgenic response.

4. DISCUSSION

In this study, we examined whether increased transcriptional activity of Sp1 caused early skeletal muscle cholesterol accumulation and insulin resistance in C57BL/6NJ mice fed a HF diet for 1 week. We found that

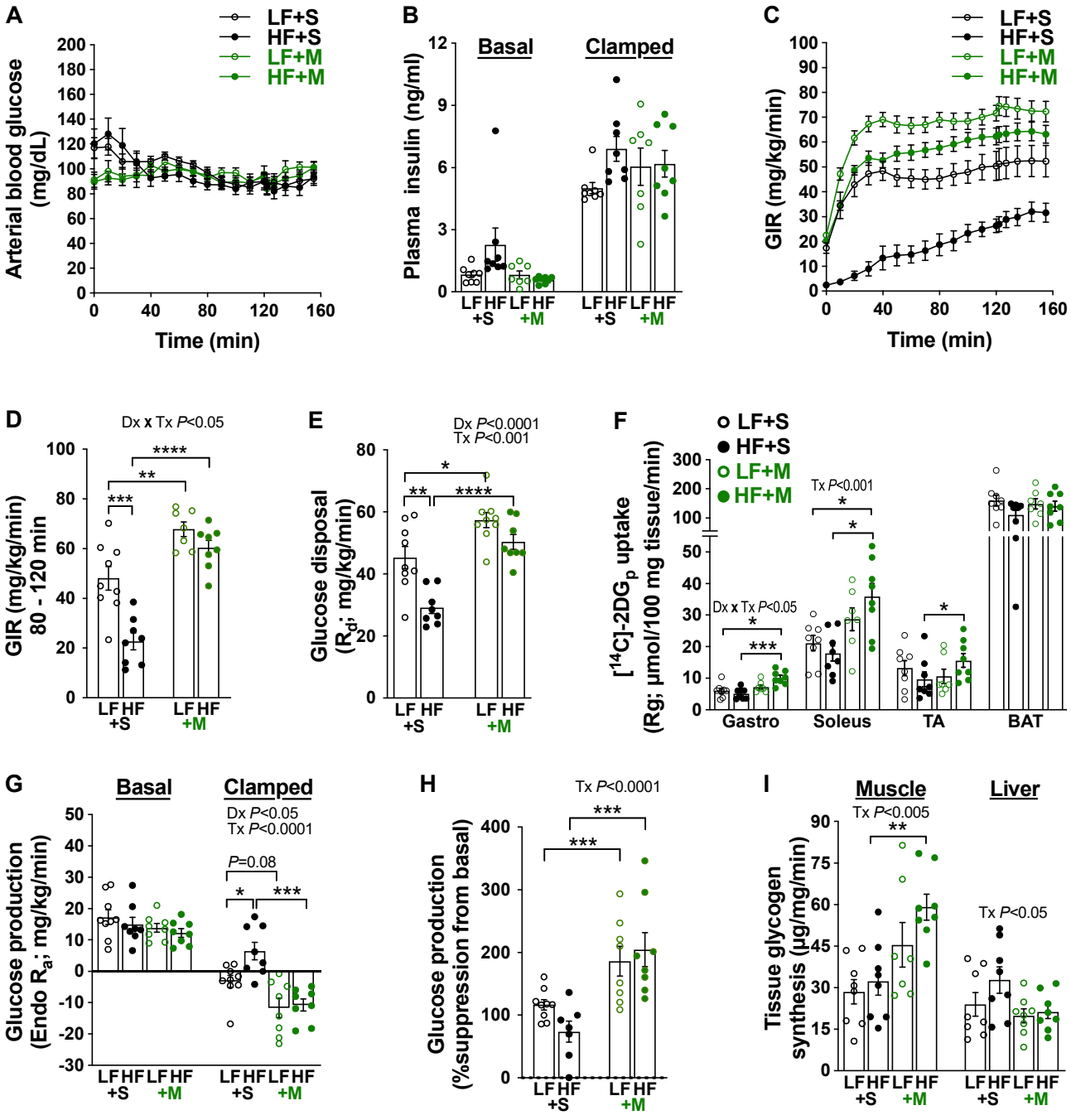

Figure 3: Daily MTM treatment prevented the development of insulin resistance in mice fed a HF diet for 1 week. (A) Arterial blood glucose, (B) plasma insulin, (C—D) Glucose infusion rate (GIR), (E) glucose disposal (R_d), (F) [^{14}C]-2DG tissue glucose uptake (R_g), (G—H) glucose production (Endo R_a) and as %suppression from basal, and (I) tissue glycogen synthesis during the hyperinsulinemic-euglycemic clamp. Data represent means ± SEM from 7 to 9 mice per group. Difference between groups was analyzed using a two-way ANOVA and Tukey's multiple comparison tests. *p < 0.05, **p < 0.005, ***p < 0.0005, ****p < 0.0001.

treating the mice with MTM daily during the 1-week HF diet exposure prevented diet-induced increases in Sp1 binding to HMGCR promoter, HMGCR expression, and PM cholesterol content. We also observed that MTM treatment protected against cortical F-actin loss that occurs with diet-induced PM cholesterol accumulation. Consistent with an essential role of this actin network for insulin-regulated glucose transport [3—6], we observed a marked increase in glucose disposal and skeletal muscle glucose uptake in MTM-treated HF-fed mice. This was associated with a significant increase in skeletal muscle glycogen synthesis. While we did not observe an effect of MTM on brown adipose tissue glucose uptake, we did observe that MTM restored hepatic insulin resistance that developed during the 1-week HF diet. Future studies will test if changes in liver gene expression restored insulin-stimulated suppression of endogenous glucose production or are a result of changes in insulin sensitivity.

In accordance with these beneficial effects of MTM, we previously found that MTM protected against HBP-induced insulin resistance in 3T3-L1 adipocytes [12]. Those previous *in vitro* studies identified that

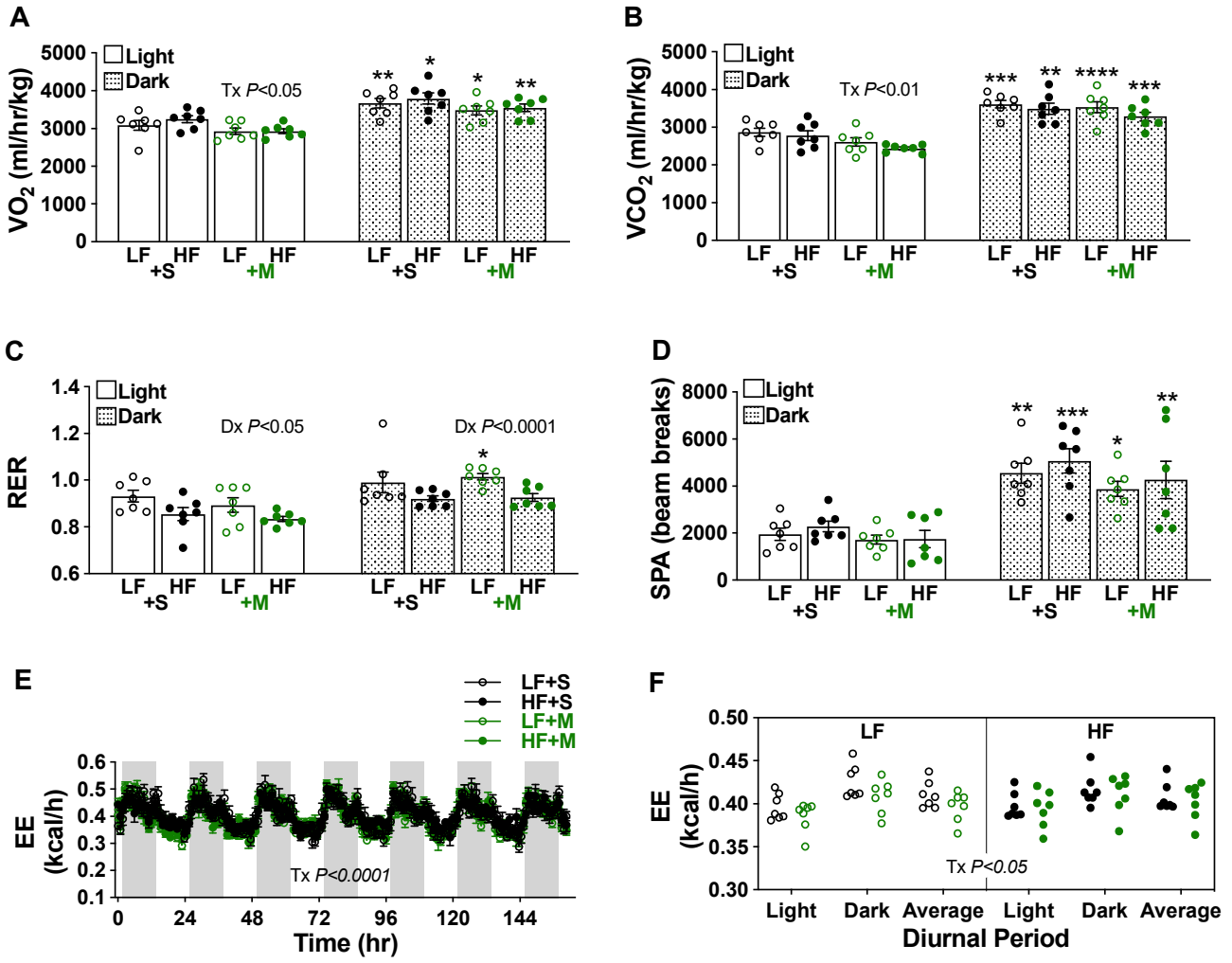

Figure 4: Metabolic function and energy expenditure in mice during the diet/intervention. (A) Oxygen consumption (VO2), (B) carbon dioxide production (VCO2), (C) respiration (RER), (D) spontaneous physical activity (SPA), and (E–F) energy expenditure (EE). Data represent means ± SEM from 7 mice per group. (A–D) Difference between groups was analyzed using a two-way ANOVA and Tukey's multiple comparison tests. *p < 0.05, **p < 0.005, ***p < 0.0005, ****p < 0.0001 versus respective light group.

increased HBP activity stimulated the same Sp1 cholesterolgenic transcriptional activity, F-actin loss, and insulin resistance. In this current study, we found that HF feeding increased HBP-mediated *O*-GlcNAcylation of Sp1. Because our previous experiments demonstrated that *O*-GlcNAc-Sp1 levels were not affected by MTM [12], the beneficial effect of MTM on preventing 'membrane/cytoskeletal' insulin resistance in HF-fed mice is likely a result of reduced Sp1/DNA binding, not reduced Sp1 *O*-GlcNAcylation. This drug is known to be highly selective to GC-rich sequences of DNA, competitively inhibiting Sp1 binding without affecting the binding of other Sp1 family members (49). In further agreement with a role of the HBP in this Sp1 cholesterolgenic mechanism of insulin resistance, we found that skeletal muscle overexpression of GFAT increased PM cholesterol. Previous characterization of our GFAT Tg mice using hyperinsulinemic-euglycemic clamp technique confirmed that male and female Tg mice develop insulin resistance [23]. Finding that skeletal muscle from saline-, but not MTM-, treated Tg mice had increases in HMGCR expression and PM cholesterol compared to saline-treated Wt littermate control mice suggest that the HBP/Sp1 cholesterolgenic response in these mice could contribute to their documented insulin resistance. It is of clinical interest that there is an inverse correlation between human skeletal muscle PM cholesterol and whole-body glucose disposal [11], and that GFAT activity is increased in skeletal muscle of patients with T2D [37]. Further, ~2-fold elevations in mRNA and protein content of GFAT, with associated gains in UDP-GlcNAc and increased Sp1 binding to DNA have been observed in palmitate-induced insulin-resistant human skeletal muscle [38]. In accordance, we found increased HBP activity and HMGCR expression, excess PM cholesterol accumulation and cortical F-actin loss in palmitate-induced insulin-resistant L6 myotubes [11].

As noted earlier, proximal insulin signaling proteins such as Akt are subject to HBP-mediated *O*-GlcNAcylation [20]; however, removal of the *O*-GlcNAc moieties from Akt is ineffective in mitigating HBP-induced insulin resistance [26]. These findings agree with a growing appreciation that generalized impairments in insulin signaling because of a defect in one or more proximal insulin signaling components cannot explain diet-induced insulin resistance [39]. In support of a distal mechanism of diet-induced insulin resistance, gastrocnemius skeletal muscles obtained from saline-treated HF-fed mice at the termination of the hyperinsulinemic-euglycemic clamp did not show impaired phosphorylation of Akt compared to saline-treated LF-fed mice, nor did MTM treatment of these mice enhance the phosphorylation status of Akt (see

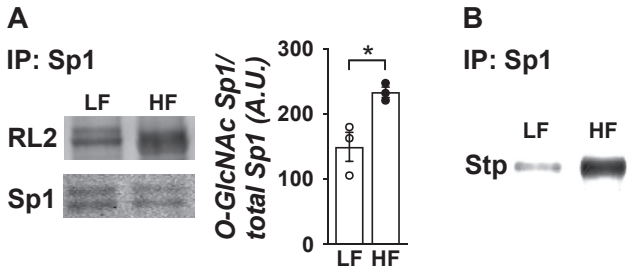

Figure 5: One week of HF feeding provokes *O*-linked glycosylation of Sp1 in skeletal muscle. Lysates from skeletal muscle from LF- and HF-fed mice were immunoprecipitated with an Sp1 antibody to detect *O*-linked glycosylation. (A) Eluted samples were immunoblotted (IB) with RL2 or Sp1 antibody (n = 3 per group). (B) Immunoprecipitates were subjected to enzymatic biotin labeling with a Click-iT kit and immunoblotted with streptavidin (Stp) antibody (n = 3 per group). Note Sp1 antibody labeling of the biotin-labeled O-GlcNAc did not yield interpretable immunoblots. Representable immunoblots are shown. Data represent means ± SEM. Difference between groups was analyzed using a two-tailed unpaired t test. *p < 0.05.

Supplemental Fig. 2). Because insulin resistance is detected at sub-maximal and maximal insulin doses in humans [40], observing a marked loss of glucose disposal despite unaffected insulin signaling to Akt implicates a distal localized mechanism of diet-induced insulin resistance. Loss of cortical actin filaments, which impairs insulin-stimulated GLUT4 regulation in HF-fed mice [2], was confirmed in the current study and was fully mitigated by MTM.

Some aspects of the current study need to be considered. First, we individually housed the C57BL/6NJ mice because of reported aggression within this 6 N line [41]. Therefore, it is possible that the stress of being individually housed could affect the diet-induced mechanism of insulin resistance. However, we have observed PM cholesterol accumulation and cortical F-actin loss in skeletal muscle from C57BL/6 J mice that were either singly- or grouped-housed following an 8-week HF diet [11,42]. We have also reported similar outcomes in cells cultured under a variety of physiologically-relevant conditions that increase HBP activity [11–13]. We have also uniformly measured excess skeletal muscle cholesterol accumulation in insulin-resistant mice, rats, swine, and humans [11,43]. In aggregate, these findings suggest that any stress induced by being individually housed likely did not affect this diet-induced mechanism of insulin resistance. Second, although the typical range for fasting glucose in mice is 135–160 mg/dL, we clamped mice at 90 mg/dL. Our rationale for choosing this euglycemic setpoint for our studies is reflective of the observed glycemia in our mice at the end of the baseline tracer infusion period, a practice we and others have reported [32,33,44,45]. Implications of clamping mice at this glycemia are that we are measuring whole-body glucose metabolism at physiological levels that they are experiencing daily. A limitation of this strategy is that we may be inducing subtle counter-regulatory responses in some animals. However, robust glucose infusion rates in all groups excluding the saline-treated HF-fed group suggest that this is not a primary driver of the observed effects. Moreover, pilot data from mice without tracer that were clamped at 110 mg/dL showing nearly identical findings also support subtle

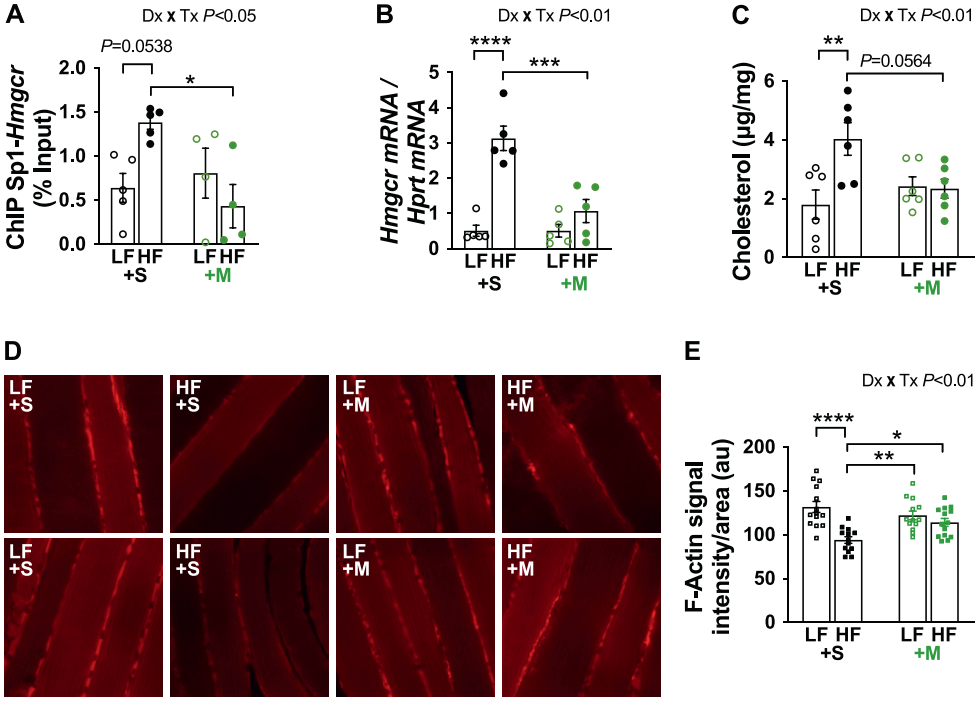

Figure 6: One week of HF feeding causes a cholesterolgenic response in skeletal muscle. (A) ChIP was performed on skeletal muscle lysates. Purified DNA and primers specific to the Sp1-binding sites in the promoter region of *Hmgcr* were used for qPCR (n = 4–5 per group). (B) *Hmgcr* mRNA expression (n = 5 per group). (C) Triad-enriched membrane cholesterol (n = 6 per group). (D) Two representative images of 1-mm sections of soleus muscle per group subjected to immunofluorescent labeling of F-actin. Note prior to imaging, all samples were de-identified to ensure an objective analysis. All images were taken in the same focal plane of the section and under identical microscopic parameters. (E) Immunofluorescence F-actin intensity/area for multiple (3–5) images captured in muscle sections per muscle per mouse (n = 3). Difference between groups was analyzed using a two-way ANOVA and Tukey's multiple comparison tests. *p < 0.05, **p < 0.005, ***p < 0.0005, ****p < 0.0001.

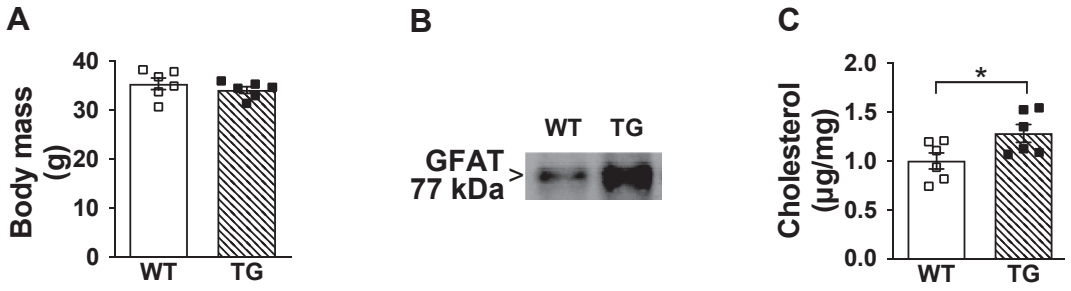

Figure 7: Overexpression of skeletal muscle GFAT causes membrane cholesterol accumulation and glucose intolerance in male mice fed standard laboratory chow. (A) Body mass of age-and weight-matched GFAT Tg and Wt littermate control mice (n = 6 per group), (B) Representative immunoblot of GFAT from skeletal muscle lysate, and (C) Skeletal muscle membrane cholesterol (n = 6 per group) from these mice. Data represent means ± SEM. Difference between groups was analyzed using a one-tailed unpaired t test. *p < 0.05.

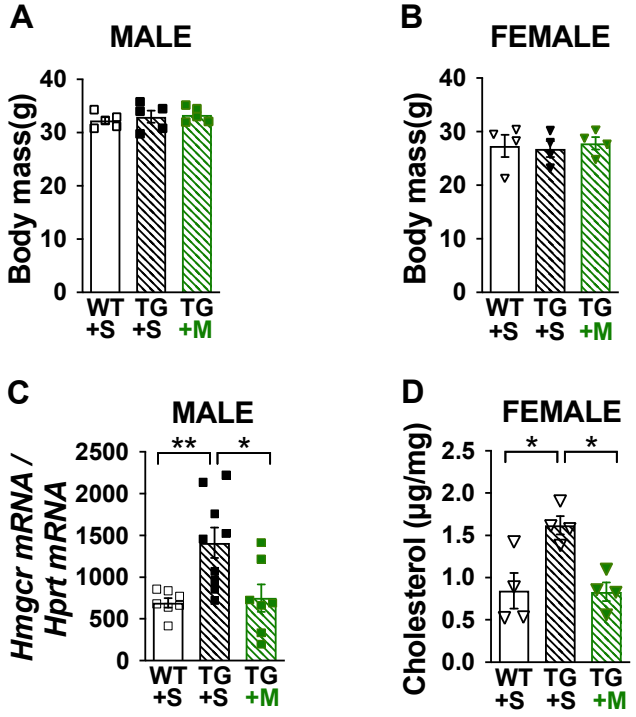

Figure 8: Insulin-resistant GFAT Tg mice display an Sp1-mediated cholesterolgenic response. Age- and weight-matched male and female Tg and Wt littermate control mice fed standard laboratory chow were treated with either saline (+S) or MTM (+M) for 1 wk for determination of (A, B) Body mass (4–5 per group), (C) Skeletal muscle *Hmgcr* mRNA expression (n = 7–9 per group), and (D) Skeletal muscle membrane cholesterol (n = 4). Data represent means ± SEM. Difference between groups was analyzed using a one-way ANOVA and the Tukey's multiple comparison tests. *p < 0.05, **p < 0.005.

counter-regulatory responses are likely not the driver of the observed effects (see Supplemental Fig. 3). Regardless of this nuance, the overarching observations are that HF feeding induced early insulin resistance that was reversed by MTM treatment. Third, while we measured a significant increase in skeletal muscle glucose uptake and glycogen synthesis in MTM-treated HF-fed mice, decreases in either of these measures in skeletal muscle from saline-treated HF-fed mice did not reach statistical significance. This agrees with other studies showing that measured skeletal muscle insulin resistance requires longer HF diet interventions [41,46]. However, transverse tubule membrane we prepared from mixed hindlimb skeletal muscle from these HF-fed mice 30 min after administering glucose (2 g/kg, i.p.) showed a complete loss of GLUT4 translocation, as compared to the significant stimulated increase observed in LF-fed mice [2]. This loss was dramatic considering the elevated level of insulin we and others have measured in these HF-fed animals that were i.p. administered glucose [2,41]. We found that the impaired regulation of GLUT4 translocation was completely prevented in mice where the excess skeletal muscle cholesterol was removed by treating with MβCD [2]. Although that study detected a biological action of insulin following an i.p. glucose injection in LF-fed, but not HF-fed, mice demonstrating skeletal muscle insulin resistance, it should be noted that measured rises in blood insulin concentrations after an i.p. glucose administration is largely absent compared to that measured following an oral glucose administration in mice [47]. Therefore, changes in whole-body insulin sensitivity may not be directly inferred from an i.p. GTT [47]. Our use of the hyperinsulinemic-euglycemic clamp in this study for the diet/treatment interventions and in our previous study of GFAT Tg mice [23] show that either 1 week of HF feeding or overexpression of GFAT causes insulin resistance. Because we did not perform the clamp analyses on our GFAT Tg mice in the current study, it remains to be determined if insulin sensitivity in these animals is restored by the beneficial effect of MTM on blocking HMGCR expression and PM cholesterol accumulation.

While we have shown that excess skeletal muscle cholesterol causes insulin resistance within 1 week of its buildup in the PM, we do not know if there may be an early increase in other lipids that also have the potential to impact insulin sensitivity. Also, the long-term effect of excess skeletal muscle cholesterol on insulin sensitivity needs clarification. We have found increased PM cholesterol levels in skeletal muscle following longer HF diet durations in mice (4–8 weeks) [11,42] and swine (55 weeks) [11], and in skeletal muscle from rats [43] and humans [11] with existing insulin resistance. While *ex vivo* removal of excess PM cholesterol from skeletal muscle isolated from mice fed a HF diet for 4–8 weeks, or from insulin-resistant Zucker rats markedly improved or fully restored insulin sensitivity of the isolated muscle [43,48], it is not known whether *in vivo* blockade of a long-term diabetogenic effect of the HBP/Sp1 cholesterolgenic response with MTM could prevent the development of chronic diet-induced insulin resistance.

In conclusion, our results provide innovative insight into cellular and molecular changes leading to early diet-induced insulin resistance. With fasting plasma glucose being elevated more than a decade before diagnosis of T2D, and even before prediabetes is recognized [49–52], our findings bring into view that glucose channeled through the HBP may be a basis of early skeletal muscle insulin resistance. Because it is known that glucose flux through the HBP is amplified by availability of saturated fatty acids, the risk of skeletal muscle cholesterol

accumulation might already be present at glucose concentrations below the current cut-off for prediabetes. Moreover, our prior findings that exercise [42] and caloric restriction [2] are effective in completely normalizing excess PM cholesterol content in skeletal muscle provide a fresh mechanistic perspective on how these lifestyle modifications are a cornerstone of diabetes prevention [53].

AUTHOR CONTRIBUTION

B.A.G. and J.S.E. designed the study, conducted experiments, gathered, and analyzed data, and wrote the manuscript. J.D.C., M.G.T. helped design the study, conducted experiments, gathered, and analyzed data, and write the manuscript. A.P.R and M.K. conducted experiments and gathered and analyzed data. L.T. performed chromatin immunoprecipitation analyses. T.B. helped perform mRNA expression analyses. N.D.S. conducted metabolic caging experiments and gathered and analyzed data. T.K. and K.M.H. conducted the hyperinsulinemic-euglycemic clamp studies, gathered, and analyzed data, and helped write the manuscript. D.A.M. helped design and write the manuscript. A.P.R. and J.T.B. helped write the manuscript. J.S.E. is the guarantor of this work and, as such, had full access to all the data in the study and takes responsibility for the integrity of the data and the accuracy of the data analysis.

DATA AVAILABILITY

Data will be made available on request.

ACKNOWLEDGEMENTS

Research reported in this publication was supported in part by the American Diabetes Association under Award Number 7-14-BS-053 (to J.S.E.), the National Institute of Diabetes and Digestive and Kidney Diseases (NIDDK) of the National Institutes of Health (NIH) under Award Numbers R01DK11422 (to J.S.E.), 1R01DK112934 (to K.M.H.) and T32DK064466 (to B.A.G.), the National Institute of General Medical Sciences (NIGMS) of the NIH under the Award Number T32GM077229 (to B.A.G.), a BRIDGE award from Indiana University Purdue University Indianapolis (to J.S.E), a Biomedical Research Grant award from Indiana University School of Medicine (to J.S.E), and an Elwert award in medicine (to J.S.E). The content is solely the responsibility of the authors and does not necessarily represent the official views of the Indiana University School of Medicine. Cores within the NIDDK/NIH Diabetes Research Centers under award numbers P30DK097512 and P30DK079626 also supported this work. The content is solely the responsibility of the authors and does not necessarily represent the official views of the ADA and NIH. We would like to thank Dr. Julio E. Ayala within the Department of Molecular Physiology and Biophysics at Vanderbilt University for helpful discussion on hyperinsulinemic-euglycemic clamp analyses, Anthony Acton, Kara Orr, and Lata Udari within the Center for Diabetes & Metabolic Diseases Cores at Indiana University School of Medicine for their assistance with blood insulin analyses, and Andrew Elmendorf within the Indiana Biosciences Research Institute for his assistance with tissue analyses.

CONFLICT OF INTEREST

The authors declare that they have no known competing financial interests or personal relationships that could have appeared to influence the work reported in this paper.

APPENDIX A. SUPPLEMENTARY DATA

Supplementary data to this article can be found online at https://doi.org/10.1016/j.molmet.2023.101715.

REFERENCES

[1] Norton L, Shannon C, Gastaldelli A, DeFronzo RA. Insulin: the master regulator of glucose metabolism. Metabolism 2022;129:155142.
[2] Grice BA, Barton KJ, Covert JD, Kreilach AM, Tackett L, Brozinick JT, et al. Excess membrane cholesterol is an early contributing reversible aspect of skeletal muscle insulin resistance in C57BL/6NJ mice fed a Western-style high-fat diet. Am J Physiol Endocrinol Metab 2019;317(2):E362–73.
[3] Tsakiridis T, Vranic M, Klip A. Disassembly of the actin network inhibits insulin-dependent stimulation of glucose transport and prevents recruitment of glucose transporters to the plasma membrane. J Biol Chem 1994;269(47):29934–42.
[4] Omata W, Shibata H, Li L, Takata K, Kojima I. Actin filaments play a critical role in insulin-induced exocytotic recruitment but not in endocytosis of GLUT4 in isolated rat adipocytes. Biochem J 2000;346(Pt 2):321–8.
[5] Tong P, Khayat ZA, Huang C, Patel N, Ueyama A, Klip A. Insulin-induced cortical actin remodeling promotes GLUT4 insertion at muscle cell membrane ruffles. J Clin Invest 2001;108(3):371–81.
[6] Brozinick Jr JT, Hawkins ED, Strawbridge AB, Elmendorf JS. Disruption of cortical actin in skeletal muscle demonstrates an essential role of the cytoskeleton in glucose transporter 4 translocation in insulin-sensitive tissues. J Biol Chem 2004;279(39):40699–706.
[7] Besseling J, Hutten BA. Is there a link between diabetes and cholesterol metabolism? Expert Rev Cardiovasc Ther 2016;14(3):259–61.
[8] Ding J, Reynolds LM, Zeller T, Muller C, Lohman K, Nicklas BJ, et al. Alterations of a cellular cholesterol metabolism network are a molecular feature of obesity-related type 2 diabetes and cardiovascular disease. Diabetes 2015;64(10):3464–74.
[9] Fall T, Xie W, Poon W, Yaghootkar H, Magi R, Consortium G, et al. Using genetic variants to assess the relationship between circulating lipids and type 2 diabetes. Diabetes 2015;64(7):2676–84.
[10] Grice BA, Elmendorf JS. New aspects of cellular cholesterol regulation on blood glucose control: a review and perspective on the impact of statin medications on metabolic health. US Endocrinol 2017;13(2):63–8.
[11] Habegger KM, Penque BA, Sealls W, Tackett L, Bell LN, Blue EK, et al. Fat-induced membrane cholesterol accrual provokes cortical filamentous actin destabilisation and glucose transport dysfunction in skeletal muscle. Diabetologia 2012;55(2):457–67.
[12] Penque BA, Hoggatt AM, Herring BP, Elmendorf JS. Hexosamine biosynthesis impairs insulin action via a cholesterolgenic response. Mol Endocrinol 2013;27(3):536–47.
[13] Bhonagiri P, Pattar GR, Habegger KM, McCarthy AM, Tackett L, Elmendorf JS. Evidence coupling increased hexosamine biosynthesis pathway activity to membrane cholesterol toxicity and cortical filamentous actin derangement contributing to cellular insulin resistance. Endocrinology 2011;152(9):3373–84.
[14] Marshall S, Bacote V, Traxinger RR. Discovery of a metabolic pathway mediating glucose-induced desensitization of the glucose transport system. Role of hexosamine biosynthesis in the induction of insulin resistance. J Biol Chem 1991;266(8):4706–12.
[15] McClain DA, Crook ED. Hexosamines and insulin resistance. Diabetes 1996;45(8):1003–9.
[16] Buse MG. Hexosamines, insulin resistance, and the complications of diabetes: current status. Am J Physiol Endocrinol Metab 2006;290(1):E1–8.
[17] Kreppel LK, Blomberg MA, Hart GW. Dynamic glycosylation of nuclear and cytosolic proteins. Cloning and characterization of a unique O-GlcNAc transferase with multiple tetratricopeptide repeats. J Biol Chem 1997;272(14):9308–15.
[18] Lubas WA, Frank DW, Krause M, Hanover JA. O-Linked GlcNAc transferase is a conserved nucleocytoplasmic protein containing tetratricopeptide repeats. J Biol Chem 1997;272(14):9316–24.

[19] Hart GW. Three decades of research on O-GlcNAcylation - a major nutrient sensor that regulates signaling, transcription and cellular metabolism. Front Endocrinol 2014;5:183.
[20] Ma J, Hart GW. Protein O-GlcNAcylation in diabetes and diabetic complications. Expert Rev Proteomics 2013;10(4):365–80.
[21] Vaidyanathan K, Wells L. Multiple tissue-specific roles for the O-GlcNAc post-translational modification in the induction of and complications arising from type II diabetes. J Biol Chem 2014;289(50):34466–71.
[22] Cooksey RC, Hebert Jr LF, Zhu JH, Wofford P, Garvey WT, McClain DA. Mechanism of hexosamine-induced insulin resistance in transgenic mice overexpressing glutamine:fructose-6-phosphate amidotransferase: decreased glucose transporter GLUT4 translocation and reversal by treatment with thiazolidinedione. Endocrinology 1999;140(3):1151–7.
[23] Hebert Jr LF, Daniels MC, Zhou J, Crook ED, Turner RL, Simmons ST, et al. Overexpression of glutamine:fructose-6-phosphate amidotransferase in transgenic mice leads to insulin resistance. J Clin Invest 1996;98(4):930–6.
[24] McClain DA, Lubas WA, Cooksey RC, Hazel M, Parker GJ, Love DC, et al. Altered glycan-dependent signaling induces insulin resistance and hyperleptinemia. Proc Natl Acad Sci U S A 2002;99(16):10695–9.
[25] Kralik SF, Liu P, Leffler BJ, Elmendorf JS. Ceramide and glucosamine antagonism of alternate signaling pathways regulating insulin- and osmotic shock-induced glucose transporter 4 translocation. Endocrinology 2002;143(1):37–46.
[26] Robinson KA, Ball LE, Buse MG. Reduction of O-GlcNAc protein modification does not prevent insulin resistance in 3T3-L1 adipocytes. Am J Physiol Endocrinol Metab 2007;292(3):E884–90.
[27] Ross SA, Chen X, Hope HR, Sun S, McMahon EG, Broschat K, et al. Development and comparison of two 3T3-L1 adipocyte models of insulin resistance: increased glucose flux vs glucosamine treatment. Biochem Biophys Res Commun 2000;273(3):1033–41.
[28] Chung SS, Choi HH, Cho YM, Lee HK, Park KS. Sp1 mediates repression of the resistin gene by PPARgamma agonists in 3T3-L1 adipocytes. Biochem Biophys Res Commun 2006;348(1):253–8.
[29] Sleiman SF, Langley BC, Basso M, Berlin J, Xia L, Payappilly JB, et al. Mithramycin is a gene-selective Sp1 inhibitor that identifies a biological intersection between cancer and neurodegeneration. J Neurosci 2011;31(18):6858–70.
[30] Fekedulegn DB, Andrew ME, Burchfiel CM, Violanti JM, Hartley TA, Charles LE, et al. Area under the curve and other summary indicators of repeated waking cortisol measurements. Psychosom Med 2007;69(7):651–9.
[31] Pruessner JC, Kirschbaum C, Meinlschmid G, Hellhammer DH. Two formulas for computation of the area under the curve represent measures of total hormone concentration versus time-dependent change. Psychoneuroendocrinology 2003;28(7):916–31.
[32] Kim T, Holleman CL, Nason S, Arble DM, Ottaway N, Chabenne J, et al. Hepatic glucagon receptor signaling enhances insulin-stimulated glucose disposal in rodents. Diabetes 2018;67(11):2157–66.
[33] Kim T, Nason S, Antipenko J, Finan B, Shalev A, DiMarchi R, et al. Hepatic mTORC2 signaling facilitates acute glucagon receptor enhancement of insulin-stimulated glucose homeostasis in mice. Diabetes 2022;71(10):2123–35.
[34] Finegood DT, Bergman RN, Vranic M. Estimation of endogenous glucose production during hyperinsulinemic-euglycemic glucose clamps. Comparison of unlabeled and labeled exogenous glucose infusates. Diabetes 1987;36(8):914–24.
[35] Cobelli C, Mari A, Ferrannini E. Non-steady state: error analysis of Steele's model and developments for glucose kinetics. Am J Physiol 1987;252(5 Pt 1):E679–89.
[36] Hidalgo C, Jorquera J, Tapia V, Donoso P. Triads and transverse tubules isolated from skeletal muscle contain high levels of inositol 1,4,5-trisphosphate. J Biol Chem 1993;268(20):15111–7.
[37] Yki-Jarvinen H, Daniels MC, Virkamaki A, Makimattila S, DeFronzo RA, McClain D. Increased glutamine:fructose-6-phosphate amidotransferase activity in skeletal muscle of patients with NIDDM. Diabetes 1996;45(3):302–7.
[38] Weigert C, Klopfer K, Kausch C, Brodbeck K, Stumvoll M, Haring HU, et al. Palmitate-induced activation of the hexosamine pathway in human myotubes: increased expression of glutamine:fructose-6-phosphate aminotransferase. Diabetes 2003;52(3):650–6.
[39] Fazakerley DJ, Krycer JR, Kearney AL, Hocking SL, James DE. Muscle and adipose tissue insulin resistance: malady without mechanism? J Lipid Res 2019;60(10):1720–32.
[40] DeFronzo RA, Tripathy D. Skeletal muscle insulin resistance is the primary defect in type 2 diabetes. Diabetes Care 2009;32(Suppl 2):S157–63.
[41] Fisher-Wellman KH, Ryan TE, Smith CD, Gilliam LA, Lin CT, Reese LR, et al. A direct comparison of metabolic responses to high fat diet in C57BL/6J and C57BL/6NJ mice. Diabetes 2016;65(11):3249–61.
[42] Ambery AG, Tackett L, Penque BA, Brozinick JT, Elmendorf JS. Exercise training prevents skeletal muscle plasma membrane cholesterol accumulation, cortical actin filament loss, and insulin resistance in C57BL/6J mice fed a western-style high-fat diet. Phys Rep 2017;5(16).
[43] Habegger KM, Hoffman NJ, Ridenour CM, Brozinick JT, Elmendorf JS. AMPK enhances insulin-stimulated GLUT4 regulation via lowering membrane cholesterol. Endocrinology 2012;153(5):2130–41.
[44] Qiao A, Zhou J, Xu S, Ma W, Boriboun C, Kim T, et al. Sam68 promotes hepatic gluconeogenesis via CRTC2. Nat Commun 2021;12(1):3340.
[45] Alquier T, Poitout V. Considerations and guidelines for mouse metabolic phenotyping in diabetes research. Diabetologia 2018;61(3):526–38.
[46] Turner N, Kowalski GM, Leslie SJ, Risis S, Yang C, Lee-Young RS, et al. Distinct patterns of tissue-specific lipid accumulation during the induction of insulin resistance in mice by high-fat feeding. Diabetologia 2013;56(7):1638–48.
[47] Small L, Ehrlich A, Iversen J, Ashcroft SP, Trost K, Moritz T, et al. Comparative analysis of oral and intraperitoneal glucose tolerance tests in mice. Mol Metabol 2022;57:101440.
[48] Llanos P, Contreras-Ferrat A, Georgiev T, Osorio-Fuentealba C, Espinosa A, Hidalgo J, et al. The cholesterol-lowering agent methyl-beta-cyclodextrin promotes glucose uptake via GLUT4 in adult muscle fibers and reduces insulin resistance in obese mice. Am J Physiol Endocrinol Metab 2015;308(4):E294–305.
[49] Tabak AG, Jokela M, Akbaraly TN, Brunner EJ, Kivimaki M, Witte DR. Trajectories of glycaemia, insulin sensitivity, and insulin secretion before diagnosis of type 2 diabetes: an analysis from the Whitehall II study. Lancet 2009;373(9682):2215–21.
[50] Mason CC, Hanson RL, Knowler WC. Progression to type 2 diabetes characterized by moderate then rapid glucose increases. Diabetes 2007;56(8):2054–61.
[51] Weyer C, Bogardus C, Mott DM, Pratley RE. The natural history of insulin secretory dysfunction and insulin resistance in the pathogenesis of type 2 diabetes mellitus. J Clin Invest 1999;104(6):787–94.
[52] Shiffman D, Tong CH, Rowland CM, Devlin JJ, Meigs JB, McPhaul MJ. Elevated hemoglobin A1c is associated with incident diabetes within 4 Years among normoglycemic, working-age individuals in an employee wellness program. Diabetes Care 2018;41(6):e99–100.
[53] Tabak AG, Herder C, Rathmann W, Brunner EJ, Kivimaki M. Prediabetes: a high-risk state for diabetes development. Lancet 2012;379(9833):2279–90.

